More on Large Q^2 Events with Polarized Beams

Junya HASHIDA and Yuichiro KIYO

Deptartment of Physics, Hiroshima University, Higashi-Hiroshima 739-8526, Japan

(Received August 24, 1998)

We discuss polarized proton-positron scattering in the context of the excess of large Q^2 events at HERA. We define and estimate a polarized asymmetry to examine two scenarios, the contact interaction and the stop scenario with broken R-parity. This asymmetry exhibits a characteristic behavior depending on the scenarios. Thus the polarized experiment at HERA will provide with a good test for these models.

arXiv:hep-ph/9808358v2 23 Feb 1999

In 1997, an event excess in the neutral current process $e^+p \to e'^+X$ in the region of high momentum transfer $Q^2 \geq 15,000$ GeV^2 was reported by H1 and ZEUS at HERA [1]. The observed cross section was $0.71^{+0.14}_{-0.12}$ pb, whereas the standard model (SM) predicts 0.49 pb. The new data [2] analyzed in 1998 are in agreement with the SM up to $Q^2 \simeq 10,000$ GeV^2. The excess at $Q^2 \geq 20,000$ GeV^2 is not confirmed by the new data but is still present. The present situation is rather vague, [2-4] and it is still an open question whether this is really an anomalous event or if it just results from statistical fluctuation. If the excess is not just a statistical fluctuation, it must be an indication of new interactions beyond the SM, because it appears to be very difficult to explain the data in the framework of the SM.

There have appeared many proposals and analyses of this problem. New contact interactions (CI) stemming from high energy scale physics have been analyzed, [5-7] and supersymmetric (SUSY) models with R-parity violating ($\not{R}_p$) interactions have also been discussed. [5] The two-stop scenario, [8] left stop $\tilde{t}_L$ is a mixture of the almost degenerate mass eigenstates of $\tilde{t}_1$ and $\tilde{t}_2$, with $\not{R}_p$ interactions was proposed as one of the candidates to explain broad mass distribution in the data.

HERA will begin a polarized experiment, [9] polarized proton $p(\uparrow / \downarrow)$ and lepton (positron in our discussion) scattering, in the near future. The polarized experiment is important because the polarization of the proton and lepton beams make it possible to test the chiral structure of the interactions. [10] Thus it is interesting to ask what HERA will teach us about the models in the future polarized program.

In this paper, we examine two scenarios, the CI and the two-stop scenarios in the context of the large Q^2 events at the polarized HERA. Our interest is in determining how we can examine these scenarios and what the characteristics of the models are. Thus we discuss these scenarios with regard to the future polarized experiment $e^+p(\uparrow / \downarrow) \to e^{+\prime}X$. After giving the model Lagrangians, we calculate the parton level cross sections which will be convoluted with parton distributions to form the physical cross section.

typeset using $\mathcal{PTP}$TEX.sty <ver.0.8>

The Lagrangian for the CI [5)-7)] assumes the form

$$L_{CI} = \frac{4\pi}{\Lambda^2} \sum_{\substack{q=u,d \\ a,b=L,R}} \eta^q_{ab} \left(\bar{e}_a \gamma^\mu e_a\right) \left(\bar{q}_b \gamma_\mu q_b\right), \tag{1}$$

which is the effective interaction of a certain underlying high energy physics describing low energy phenomena in the neutral current process. The subscript $R(L)$ denotes the chirality of the fields, $\eta^q_{ab} = \pm 1, 0$, and Λ is the mass scale of a heavy particle which might be exchanged among quarks and leptons. Thus these interactions are suppressed by the mass scale of the new physics, and some constraints [2), 11)] have been obtained for Λ in many experiments. The superpotential, for the stop scenario with $\not{R}_p$ interaction [5), 8)], is given by

$$W_{\not{R}} = \lambda'_{131} L_1 Q_3 D^c_1, \tag{2}$$

where L_1 and Q_3 are the superfields of the $SU(2)_L$ lepton and quark doublet, respectively, and D^c_1 is the singlet down type quark. Here the subscripts 1, 2 and 3 are the generation indices. The interaction Lagrangian can be obtained from the superpotential

$$L_{\lambda'} = \lambda'_{131} \left(\tilde{t}_L \bar{d} P_L e + \tilde{e}_L \bar{d} P_L t + \bar{\tilde{d}}_R \bar{e}^c P_L t - \tilde{b}_L \bar{d} P_L \nu_e - \tilde{\nu}_L \bar{d} P_L b - \bar{\tilde{d}}_R \bar{\nu}^c_e P_L b \right) + h.c. \tag{3}$$

For the scalar fields, $R(L)$ denotes the chirality of their superpartners. We discuss the proton-positron scattering, so only the first term $\tilde{t}_L \bar{d} P_L e + h.c.$ is relevant. In the two-stop scenario, the left stop $\tilde{t}_L$ is the superposition of the two mass eigenstates $\tilde{t}_1$ and $\tilde{t}_2$ with the mixing angle θ_t; namely $\tilde{t}_L = \tilde{t}_1 \cos\theta_t - \tilde{t}_2 \sin\theta_t$. The stop $\tilde{t}_L$ can couple only to the left handed lepton field e_L and the right handed down quark d_R. This is an important point in our discussion, because the polarized experiment can distinguish the chiral structure of the interactions in the parton-lepton scattering.

The partonic cross sections $\hat{\sigma}$ for the models are given by

$$\begin{aligned} \frac{d\hat{\sigma}(e^+_I f_J)}{dx_B dQ^2} = \delta(x_B - x) \frac{(4\pi\alpha_e)^2}{8\pi \left(\hat{s}\ Q^2\right)^2} \left[(1 + I \cdot J)\hat{s}^2 + (1 - I \cdot J)\hat{u}^2 \right] \\ \times \left| Q_\gamma(e) Q_\gamma(f) + \frac{Q^{-I}_Z(e) Q^J_Z(f)}{\sin^2\theta_W} \frac{Q^2}{Q^2 + M^2_Z} + \Delta \right|^2, \end{aligned} \tag{4}$$

where $I(J) = \pm$ correspond to the helicities $\pm 1/2$ of the positron (quark), x_B is the Bjorken variable and x is the momentum fraction of the parton, $\alpha_e = e^2/(4\pi)$, θ_W is the electro-weak angle, and $\hat{s}$ and $\hat{u}$ are the Mandelstam variables with respect to the parton-positron system, which are defined by $\hat{s} = xs$ and $\hat{u} = xu$. Δ is the contribution from the CI or $\not{R}_p$ interaction. We neglect the masses of the quarks and positron in this paper. The coupling constants of the electron and up and down quarks to the photon and Z boson are given by

$$Q_\gamma(e) = -1, \quad Q^+_Z(e) = \frac{\sin^2\theta_W}{\cos^2\theta_W}, \quad Q^-_Z(e) = \frac{2\sin^2\theta_W - 1}{2\cos\theta_W}, \tag{5}$$

$$Q_\gamma(u) = \frac{2}{3}, \quad Q_Z^+(u) = \frac{-2\sin^2\theta_W}{3\cos\theta_W}, \quad Q_Z^-(u) = \frac{3-4\sin^2\theta_W}{6\cos\theta_W}, \tag{6}$$

$$Q_\gamma(d) = \frac{-1}{3}, \quad Q_Z^+(d) = \frac{\sin^2\theta_W}{3\cos^2\theta_W}, \quad Q_Z^-(d) = \frac{-3+2\sin^2\theta_W}{6\cos\theta_W}. \tag{7}$$

For the CI scenario, Δ is given by

$$\Delta(Q^2) = -\frac{Q^2\eta^q_{-IJ}}{\alpha_e\Lambda^2}, \tag{8}$$

where the subscripts + and − of the η^q_{ab} correspond respectively to R and L. The stop exchange with the $\not{R}_p$ interaction yields the following contribution

$$\Delta(\hat{s}, Q^2) = -\frac{\alpha_{131}Q^2}{2\alpha_e}\left(\frac{\cos^2\theta_t}{\hat{s}-\tilde{m}_1^2+i\tilde{m}_1\Gamma_{\tilde{t}_1}} + \frac{\sin^2\theta_t}{\hat{s}-\tilde{m}_2^2+i\tilde{m}_2\Gamma_{\tilde{t}_2}}\right) \tag{9}$$

for the $I = J = +$ channel and $f = d$. Otherwise $\Delta = 0$ in the stop scenario. Here $\alpha_{131} = \lambda'^2_{131}/(4\pi)$, $\tilde{m}_{1,2}$ and $\Gamma_{\tilde{t}_{1,2}}$ are the masses and widths of $\tilde{t}_{1,2}$ respectively.

The cross section for the polarized proton-positron scattering is obtained by convoluting the partonic cross sections with the polarized parton distribution functions. The cross section $\sigma(e^+p(\uparrow))$ for the longitudinally polarized proton $p(\uparrow)$ and positron scattering can be written:

$$\frac{d\sigma}{dx_B dQ^2}(e^+p(\uparrow)) = \int_0^1 dx \sum_f \left(\frac{d\hat{\sigma}\,(e^+f_+)}{dx_B dQ^2} f_{+/\uparrow}(x) + \frac{d\hat{\sigma}\,(e^+f_-)}{dx_B dQ^2}(x) f_{-/\uparrow}\right), \tag{10}$$

where $f_{\pm/\uparrow}(x)$ is the polarized parton distribution function for the flavor f parton with momentum fraction x and helicity $\pm 1/2$ in the proton $p(\uparrow)$.

We are interested in the region which is characterized by the two variables Q^2 and the invariant mass $M = \sqrt{\hat{s}}$, with $Q^2 \geq 20{,}000$ GeV^2 and $M \sim 200$ GeV. This corresponds to the region in which the partons in the proton have a momentum fraction $x \sim 0.4$. Thus we can safely neglect the contribution from the sea quarks, because their distribution is quite small in that region, and contributions from gluons are next to leading order in the QCD coupling constant.

In Fig.1, we show the polarized parton distributions $xu_{\pm/\uparrow}(x), xd_{\pm/\uparrow}(x)$ in the proton as a function of the momentum fraction x. The scale of the distributions is taken to be $Q^2 = 20{,}000$ GeV^2 using the parameterization of Refs.[12] and[13]. Our numerical estimation has shown that the effects of Q^2 evolutions to the parton distributions were tiny in the region considered in this paper. This is reasonable because the change in the QCD coupling constant is small for large Q^2.

One can see that most of the down quarks are oppositely polarized ($xd_+(x) \leq xd_-(x)$) with respect to the proton spin, while the up quarks are polarized along the proton spin ($xu_-(x) \leq xu_+(x)$). The largest component of the proton in the region of interest is the up quark with helicity $+1/2$. In the CI scenario, the up quarks might contribute to the large Q^2 excess if η^u_{ab} is sufficiently large. However, in the stop scenario, they can not contribute, because there is no coupling between the up

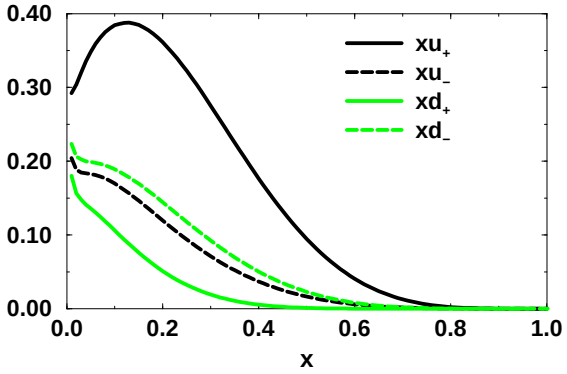

Fig. 1. The polarized parton distributions $xu_{\pm/\uparrow}(x)$ and $xd_{\pm/\uparrow}(x)$ at the scale $Q^2 = 20,000$ GeV^2.

quark and stop. The next large component is the down quark with helicity $-1/2$. This also does not couple to the stop. The situation changes if we use an oppositely polarized proton beam $p(\downarrow)$, because in this case the down quarks with helicity $+1/2$ represent the next largest component in the proton $p(\downarrow)$. Hence the cross section for $e^+p(\downarrow) \to e^{+\prime}X$ is larger than that for $e^+p(\uparrow) \to e^{+\prime}X$ in the stop scenario.

To begin with, we give numerical results for the unpolarized case. Figure 2 shows how the CI and stop scenarios explain the unpolarized HERA data.[2] The following three parameter sets for the CI scenario have been employed:

(1) $VA+ : (\eta_{LL}^{u/d}, \eta_{LR}^{u/d}, \eta_{RL}^{u/d}, \eta_{RR}^{u/d}) = (+,-,+,-)$ with $\Lambda = 2.8$ TeV,
(2) $VA- : (\eta_{LL}^{u/d}, \eta_{LR}^{u/d}, \eta_{RL}^{u/d}, \eta_{RR}^{u/d}) = (-,+,-,+)$ with $\Lambda = 2.8$ TeV,
(3) $X6- : (\eta_{LL}^{u/d}, \eta_{LR}^{u/d}, \eta_{RL}^{u/d}, \eta_{RR}^{u/d}) = (0,0,-,+)$ with $\Lambda = 1.9$ TeV,

where the 95% confidence level limits[2] on Λ obtained by the ZEUS and H1 collaborations were used. The value of Λ for the other parameter sets are very strongly constrained by the results of other experiments.[11] For the two-stop scenario, we used the values $\lambda'_{131} = 0.07, 0.05, 0.03$, $\tilde{m}_{1,2} = 200, 230$ GeV, and the stop mixing angle $\cos\theta_t = 0.5$. The branching ratios $Br(\tilde{t}_{1,2} \to e^+d)$ are 0.65 and 1.0 for $\tilde{t}_1$ and $\tilde{t}_2$, respectively.[8),14)] The parameter sets of the CI and the stop scenarios account for the unpolarized experimental data quite well. It is also seen that the behavior of the unplarized cross sections are similar in both the scenarios.

Next, we discuss the polarized case. For our purposes, it is useful to introduce the spin asymmetry $\mathcal{A}$, which is defined by

$$\mathcal{A}(Q_0^2) \equiv \frac{\int \sigma_\uparrow - \int \sigma_\downarrow}{\int \sigma_\uparrow + \int \sigma_\downarrow}, \tag{11}$$

where $\int \sigma_{\uparrow/\downarrow}$ is the integrated cross section for the polarized proton $p(\uparrow \ / \ \downarrow)$ and positron scattering. We have

$$\int \sigma_{\uparrow/\downarrow} = \int_{Q_0^2}^{Q_{max}^2} dQ^2 dx_B \ \sigma(p(\uparrow \ / \ \downarrow)e^+ \to e'^+X), \tag{12}$$

where $Q_{max}^2 = 90,000$ GeV^2.

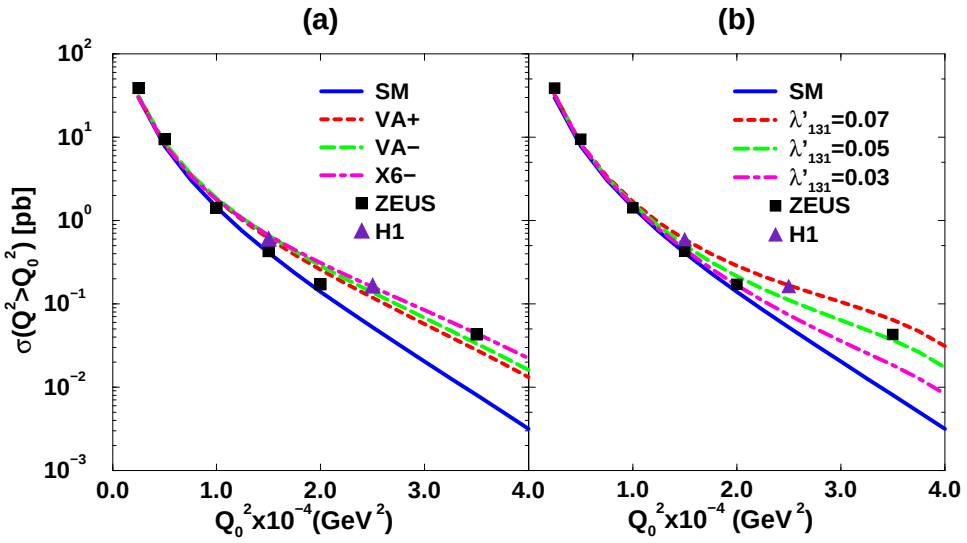

Fig. 2. The unpolarized cross sections in the range $2,500 \leq Q_0^2 \leq 40,000$ GeV^2 for (a) the CI scenario with parameter sets VA+, VA-, X6-, and (b) the two-stop scenario with $\lambda'_{131} = 0.07, 0.05, 0.03$. The solid lines indicate the cross sections predicted by the SM.

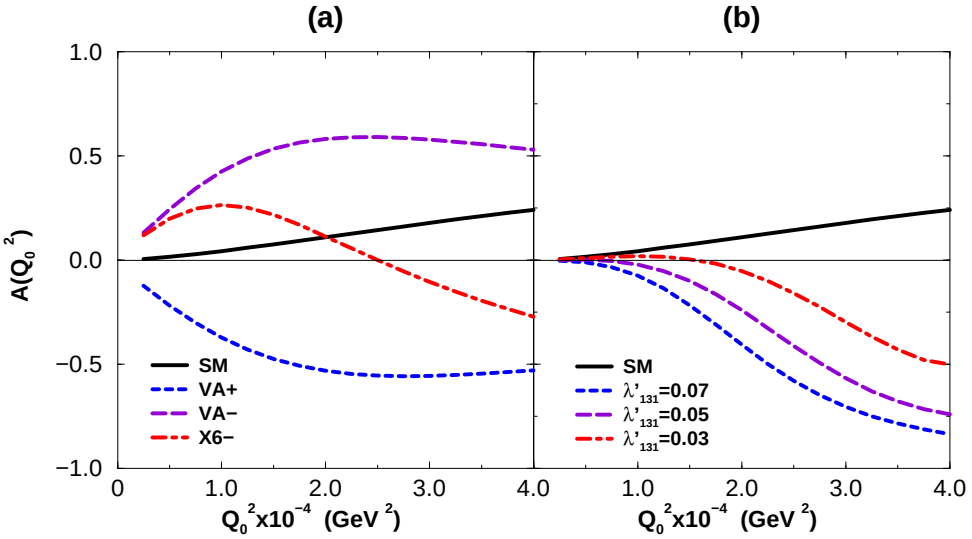

Fig. 3. The asymmetries $\mathcal{A}(Q_0^2)$ in the range $2,500 \leq Q_0^2 \leq 40,000$ GeV^2 for (a) the CI scenario with parameter sets VA+, VA-, X6-, and (b) the two-stop scenario with $\lambda'_{131} = 0.07, 0.05, 0.03$. The solid lines correspond to the prediction of the SM.

In Fig.3, we plot the spin asymmetry for the CI and two-stop scenarios. One can see that $\mathcal{A}$ in the stop scenario has a large negative value in the large Q_0^2 region, while the SM prediction is positive in the region $Q_0^2 \geq 2,500$ GeV^2. This is because the proton $p(\uparrow)$ contains more down quarks with helicity $-1/2$ than with helicity $+1/2$ and only the down quark with helicity $+1/2$ can couple to the stops which produce the large contribution to the cross sections. This is a characteristic feature

for the stop scenario with the $\not{R}_p$ interaction. A different choice for the parameters in the stop scenario does not change the results appreciably. The asymmetry for the parameter set VA+ in the CI scenario has a negative value and is similar to that in the stop scenario. However, the asymmetry for VA+ has negative value even when $Q_0^2 \sim 2,500$ GeV^2, where the asymmetry in the stop scenario is nearly zero. The asymmetries for the CI scenario are very different from that for the SM, even at $Q_0^2 \sim 2,500$ GeV^2. Hence, observing these behavior, the two scenarios may be considered distinguishable.

In summary, we discussed polarized proton-positron scattering in the context of the excess of large Q^2 events at HERA. For the CI scenario, the asymmetries $\mathcal{A}$ exhibit distinctive behavior for $Q_0^2 \sim 2,500$ GeV^2, and the value depends on the parameter sets. For the two-stop scenario, there is a characteristic dependence on Q_0^2: the value changes from zero to near -1 as Q_0^2 becomes larger. Studying this behavior at future polarized HERA will provide a good test for these models.

The authors thank to T. Nasuno, H. Tochimura and Y. Yasui for helpful discussions, and to J. Kodaira for useful comments and reading manuscript.

---

1) H1 Collaboration, Z. Phys. **C74** (1997), 191.
ZEUS Collaboration, Z. Phys. **C74** (1997), 207.
H1 and ZEUS Collaboration, B. Straub, in the Proceedings of "Lepton-Photon 97", Hamburg, 28/07/97.
2) U. F. Katz, representing the ZEUS and H1 Collaborations,
SLAC Topical Conference, Stanford, 12-14 August 1998.
http://www-h1.desy.de:80/h1/www/publications/hiq2/hiq2.html
http://www-zeus.desy.de/~ukatz/ZEUS_PUBLIC/hqex/hqex_papers.html♯Talks.
3) G. Altarelli, Nucl. Phys. **Proc. Suppl. 62** (1998), 3.
4) V. A. Noyes, *preprint* hep-ex/9707037.
5) G. Altarelli, J. Ellis, G. F. Giudice, S. Lola and M. L. Mangano, Nucl. Phys. **B506** (1997), 3.
6) V. Barger, K. Cheung, K. Hagiwara and D. Zeppenfeld, Phys. Lett. **B404** (1997), 147.
7) N. G. Deshpande, B. Dutta and X. He, Phys. Lett. **B408** (1997), 288.
8) T. Kon and T. Kobayashi, Phys. Lett. **B409** (1997), 265.
9) See, for example, A. D. Roeck and T. Gehrmann, in the proceedings of the Workshop on Deep Inelastic Scattering off Polarized Targets: Theory Meets Experiment (DESY 97-200), 523, and references therein.
10) J. M. Virey, hep-ph/9710423, in the proceedings of Workshop on Deep Inelastic Scattering off Polarized Targets: Theory Meets Experiment (DESY 97-200), 654.
11) G. Cho, K. Hagiwara and S. Matsumoto, Eur. Phys. J. **C5** (1998), 155.
CDF Coll., F. Abe et al., *Phys. Rev. Lett* **79** (1997), 2198.
OPAL Coll., G. Abbiendi et al., CERN-EP/98-108 (ICHEP98, Abs.264).
ALEPH Coll., ALEPH 98-060(19998) (ICHEP98, Abs. 906).
L3 Coll., M. Acciarri et al., CERN-EP/98-31(1998).
A. Deandrea, Phys. Lett. **B409** (1997), 277 and references therein.
12) T. Gehrmann and W. J. Stirling, Phys. Rev. **D53** (1996), 6100.
13) A. D. Martin, W. J. Stirling and R. G. Roberts, Phys. Lett. **B354** (1995), 155.
14) E. Asakawa, J. Kamoshita and A. Sugamoto. hep-ph/9803321.